Plant Ecology
https://doi.org/10.1007/s11258-023-01350-0

# Carbon allocation in an East African ant-acacia: field testing a $^{13}$C-labeling method for evaluating biotic impacts on the carbon cycle

**Gabriella M. Mizell[1,2] · Thomas Kim[3] · Benjamin W. Sullivan[4] · John S. Lemboi[2] · John Mosiany[2] · Todd M. Palmer[2,5] · Elizabeth G. Pringle[1,2]**

Received: 31 March 2023 / Accepted: 25 August 2023


**Abstract**
Tree carbon allocation is a dynamic process that depends on the tree's environment, but we know relatively little about how biotic interactions influence these dynamics. In central Kenya, the loss of vertebrate herbivores and the savanna's invasion by the ant *Pheidole megacephala* are disrupting mutualisms between the foundational tree *Acacia* (*Vachellia*) *drepanolobium* and its native ant defenders. Here, we piloted a $^{13}$Carbon (C) pulse-labeling method to investigate the influence of these biotic interactions on C allocation to ant partners by adult trees in situ. Trees withstood experimental conditions and took up sufficient labeled $^{13}CO_2$ for $^{13}$C to be detected in various C sinks, including ant mutualists. The $\delta^{13}$C in ants collected shortly after labeling suggested that trees exposed to herbivores allocated relatively more newly assimilated C to native ant defenders. Our results demonstrate the viability of the pulse-labeling method and suggest that C allocation to ant partners depends on the biotic context of the tree, but further investigation with replication is needed to characterize such differences in relation to invasion and herbivore loss.

**Keywords** $^{13}$C · *Acacia drepanolobium* · Ant–plant mutualism · Kenya · Pulse labeling

## Introduction

Trees have a major impact on the global carbon (C) cycle by influencing the balance between photosynthesis and respiration, where respiration is determined largely by tree C allocation (Trumbore 2006). Trees have complex C allocation strategies (Epron et al. 2012), which allow them to respond to their environment and, potentially, to maximize fitness over their long lifespans (Hartmann and Trumbore 2016; Huang et al. 2019, 2021). Understanding how tree C allocation varies across environmental gradients is thus necessary to predict both the dynamics of tree populations and resulting C storage in woody biomass, as well as terrestrial C fluxes. Despite the potential importance of biotic impacts on tree C allocation and resulting storage and fluxes, we have not yet accounted for the influence of biotic interactions in most models of the terrestrial C cycle (Schmitz et al. 2018).

Both the loss of herbivorous wildlife (i.e., defaunation, Dirzo et al. 2014) and the invasion of ecosystems by exotic animals are potent biotic drivers of global change that may have important impacts on tree C allocation strategies. The loss of large herbivores has well-documented impacts on plant communities (Bakker et al. 2006; Burns et al. 2009; Villar and Medici 2021), but the impacts of herbivores on C allocation by individual plants are less understood. For example, herbivory may cause plants to allocate C away from where the herbivore damage is occurring (Orians et al. 2011) or to prioritize regrowth of tissues lost to herbivores (Kristensen et al. 2020; Palacio et al. 2020). A shift in

Communicated by William Rogers.

✉ Gabriella M. Mizell
gmizell@nevada.unr.edu

1 Department of Biology, Program in Ecology, Evolution, and Conservation Biology, University of Nevada, Reno, NV, USA

2 Mpala Research Centre, Box 555-10400, Nanyuki, Kenya

3 School of Medicine, University of Nevada, Reno, NV, USA

4 Department of Natural Resources and Environmental Science, University of Nevada, Reno, NV, USA

5 Department of Biology, University of Florida, Gainesville, FL, USA

Published online: 12 September 2023

relative allocation can come at the expense of C investment in other sinks. For example, experimental herbivory simulated by shoot clipping caused oak saplings to invest more newly fixed C in above-ground regrowth, at the expense of fine roots (Palacio et al. 2020). Analogously, invasive animal species may also impact plant C allocation by changing herbivory regimes (Nuckolls et al. 2009). A better understanding of how herbivory impacts C allocation will help us integrate such stressors into our understanding of ecosystem C cycling.

Even less is known about how plant–animal interactions other than herbivory, such as mutualisms, affect C allocation. Mutualisms presumably impact tree C allocation directly by requiring the transfer of fixed C from the tree to the animal in exchange for its mutualistic service (Pringle 2016). Tree carbon allocation to symbiotic, protective ants is a phenomenon restricted to the tropics and subtropics, and we know particularly little about carbon allocation in tropical trees (Epron et al. 2012), despite their importance to the global carbon cycle (Malhi 2010). In protective mutualisms, C investment in protective partners results in protection of the tree leaves, which fix C for both plant and mutualist (Milligan et al. 2022; Pringle 2016; Pringle et al. 2013). Carbon allocation by trees to their mutualists can thus result in a long-term net C benefit to the tree, but the provisioning of C to a mutualist may also come at the expense of other sinks, like growth (Stanton and Palmer 2011). We do not yet know what proportion of the C budget of a tree is typically invested in its mutualists. Understanding the dynamics of such allocation is especially important in the face of global change, which is disrupting many mutualisms (Kiers et al. 2010).

One way to track C allocation in trees is to use isotope tracer techniques. This approach can clarify how C is allocated to mutualists by allowing the amount of the isotope tracer in the mutualists to be quantified relative to other tree sinks. Pulse-labeling experiments with the stable C isotope $^{13}C$ have become increasingly common in temperate regions (Epron et al. 2012), with some studies tracking $^{13}C$ beyond traditional tree organs (leaves, stems, roots) into belowground mutualists, like mycorrhizal fungi and microbial symbionts (Epron et al. 2011; Vandenkoornhuyse et al. 2007). Yet the typical use of a closed tent in such labeling experiments could reduce their utility in the tropics, where temperature and humidity may increase beyond photosynthetic optima, making uptake of the isotope more difficult. If these possible issues can be overcome, this method has the potential to elucidate C allocation by tropical trees, including to protective mutualists.

Here we field tested a $^{13}C$ pulse-labeling technique to study carbon allocation by a foundational tree species (*Acacia* [*Vachellia*] *drepanolobium*) in central Kenya, including allocation to its protective ant symbionts. This is an ideal system for studying C allocation in the context of mutualism because these trees are facing two major disturbances. The first is the loss of large vertebrate herbivores, which are a necessary third-party species for the persistence of the ant–plant protective interaction (Palmer et al. 2008). The second is the invasion of these savannas by *Pheidole megacephala* ants. *Pheidole megacephala* extirpates native ant species from *A. drepanolobium* trees but does not defend the trees from herbivores, leaving the trees vulnerable to catastrophic damage (Riginos et al. 2015).

By piloting pulse $^{13}C$-labeling experiments in this system, we asked (1) can *A. drepanolobium* fix pulse $^{13}CO_2$ effectively under field conditions and (2) can $^{13}C$ be detected in all identified tree C sinks? If so, we aimed to generate new hypotheses about variation in tree C allocation, including to protective mutualists, under different biotic contexts. We expected to detect $^{13}C$ in the tree's ant mutualists, especially when trees were exposed to herbivores. We did not expect to detect $^{13}C$ in invasive *P. megacephala* and predicted that the ant invasion and resulting changes in the herbivory regime would affect tree C allocation.

## Methods

### Site and study system

This study was conducted at the Ol Pejeta Conservancy (OPC; 0.03036°N, 36.96572°E), which receives approximately 900 mm of rain each year, with rainy seasons from March to May and from October to December. The site is in a savanna bushland where *A. drepanolobium* is the dominant overstory tree on clay-rich vertisol 'black cotton' soils (Wahungu et al. 2011). *Acacia drepanolobium* typically hosts one of four obligate native ant species in this system: *Crematogaster mimosae*, *Crematogaster nigriceps*, *Crematogaster sjostedti*, and *Tetraponera penzigi* (Hocking 1970). Host trees produce swollen spines to house their ants, and the three *Crematogaster* species consume extrafloral nectar produced by the tree. *Tetraponera penzigi* destroy extrafloral nectaries (Palmer et al. 2002) and may feed on fungi on host trees (Baker et al. 2017). *Crematogaster mimosae* is the most common ant mutualist, vigorously defending host trees from large herbivores, including elephants (Goheen and Palmer 2010; Stanton and Palmer 2011).

### Experimental design

We selected trees for this experiment from within a factorial experiment established in 2016 to study the impacts of the *P. megacephala* invasion at OPC. The site (Morani, 0.046301°N, 36.940110°E) comprises an active invasion front with four 50 × 50-m experimental plots, including two

invaded plots located 1 km behind the invasion front and two uninvaded plots located 1 km ahead of the invasion front. One invaded plot and one uninvaded plot were enclosed by large-herbivore exclosures (electric fences), creating a 2 × 2 factorial design of ant invasion crossed with herbivore presence.

For this trial study, we labeled one tree in each of the four plots. We chose trees of similar height (1.6 m ± 0.29) and canopy widths (1.4 m ± 0.28), pairing each tree designated for labeling with a corresponding unlabeled control tree ($n = 8$). We made the simplifying assumption that similarly sized trees were of similar ages, although we lack the data to evaluate this assumption. Control trees were located ≥10 m away from labeled trees to minimize accidental labeling.

## Pulse labeling

To label tree canopies, we constructed a whole-canopy labeling tent, made of interlocking metal poles and a high-transmittance plastic (UVA Clear Greenhouse Film, Agricultural Solutions LLC) (Fig. 1). The tent volume was 5.25 $m^3$ (1.5 × 1.75 × 2 m). Two pieces of greenhouse plastic were sealed to the base of the tree using a rubber gasket and a cam strap and clamped together along their length on each side of the base of the tree with spring clamps. These plastics excluded the ground beneath the tree from the tent, preventing direct diffusion of $^{13}CO_2$ into the soil and labeling of understory grasses. A metal frame was placed on top of these ground plastics and a third piece of plastic was

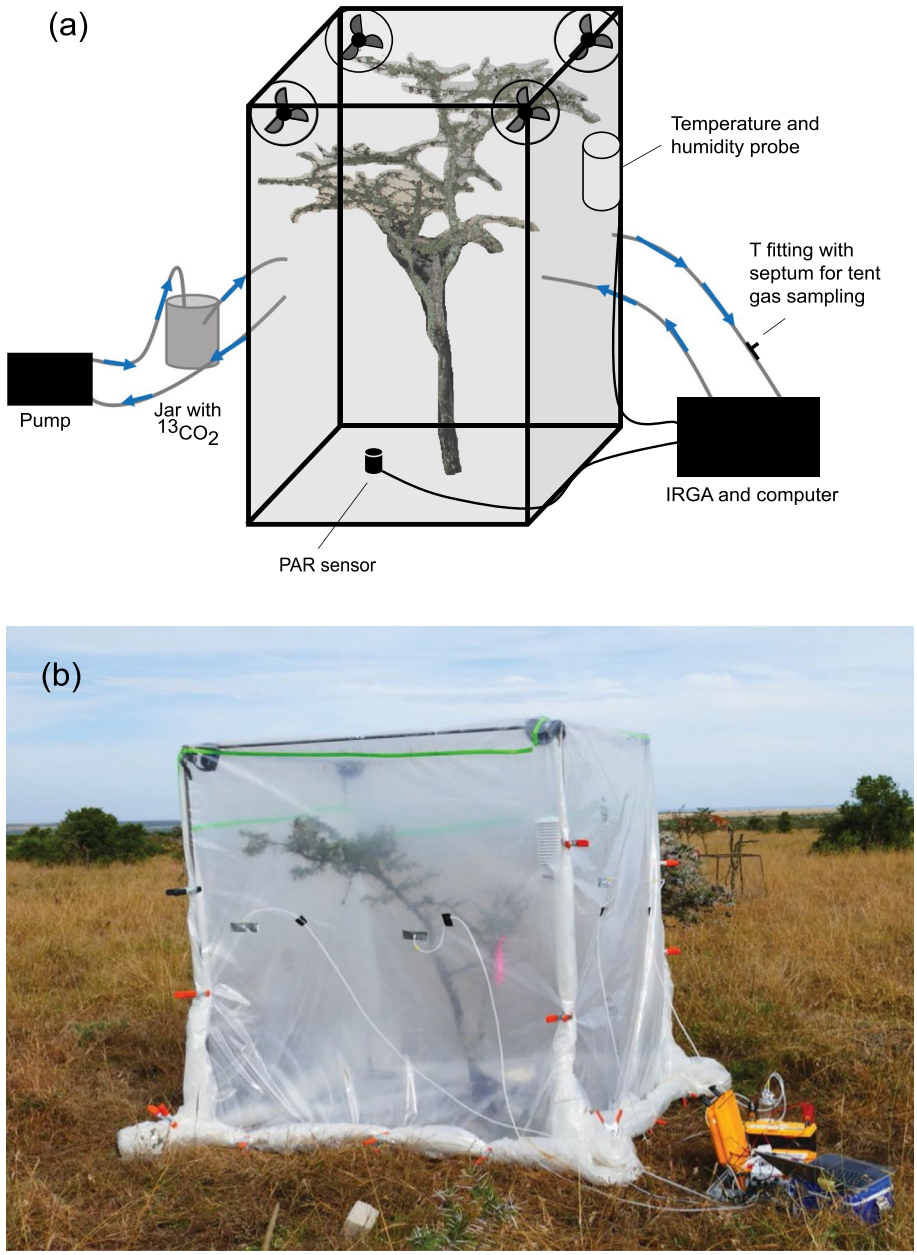


**Fig. 1** Design of the labeling chamber. **a** A schematic diagram showing the labeling chamber design. Blue arrows show the direction of airflow within the closed-system design. **b** The labeling chamber in use. There is a plastic layer on the bottom of the tent that excluded the understory grasses and soil surface

draped over the metal frame and sealed to the ground plastics (Fig. 1b). Four battery-operated 5-V 6-inch diameter fans spinning up to 2400 RPM were placed inside the tent to circulate air and evenly distribute the $^{13}CO_2$. $CO_2$ concentration, temperature, relative humidity, and photosynthetically active radiation (PAR) were monitored using a LI-8100A Infrared Gas Analyzer (hereafter "IRGA", LI-COR Inc., Lincoln, NE, USA) attached to a Vaisala HMP155 Humidity and Temperature Sensor beneath a multiplate radiation shield and to a LI-190R quantum sensor to measure PAR. Heat index was calculated from the temperature and humidity values, using equations S1 and S2 in Online Resource 1.

Labeling of *A. drepanolobium* trees with $^{13}CO_2$ occurred between March 7 and March 13, 2020. Each tree was labeled twice to add $^{13}CO_2$ from ≥14 g of $^{13}$C-sodium bicarbonate (>1100 ppm $^{13}CO_2$) to each labeling tent (Table 1). For each labeling event, we first monitored the initial $CO_2$ concentrations inside the tent after sealing it to verify net $CO_2$ uptake, indicated by a steady decline from ambient $[CO_2] = 420$ ppm to *ca*. $[CO_2] = 370$ ppm. A jar of $^{13}$C-sodium bicarbonate ($^{13}CHNaO_3$, Sigma-Aldrich 372,382) was connected to the tent via 0.25-inch Bev-a-Line plastic tubing that ran from the top of the jar to the side of the tent in a closed system (Fig. 1a). A diaphragm gas sampling 12-V pump (UNMP015KPDC-B, KNF Neuberger, Inc., Trenton, NJ) was connected in line with the jar to push the $^{13}CO_2$ out of the jar and into the tent. Once the initial $CO_2$ concentration had decreased by ~30 ppm inside the tent, we generated the $^{13}CO_2$ label by injecting 6.2% acetic acid (white vinegar) into the jar containing the $^{13}$C-sodium bicarbonate in 30-mL increments.

Incremental additions of $^{13}CO_2$ were designed to keep $CO_2$ concentrations in the tent as close as possible to atmospheric concentrations. The IRGA is optimized for $^{12}CO_2$, and trial data indicated that the IRGA detected $^{13}CO_2$ at ~33% efficiency. We used this estimate to determine when to add $^{13}CO_2$ to the tent to maintain approximately atmospheric $CO_2$ concentrations throughout the labeling period. We ended each labeling period when photosynthesis appeared to be limited by the temperature inside the tent rather than by PAR. To verify our approach to maintaining $CO_2$ concentrations and to estimate how much $^{13}CO_2$ was assimilated by the tree (see below), we took a gas sample from the tent prior to ending each labeling period. Gas was sampled from a septum on a t fitting on the tube between the tent and the IRGA (Fig. 1a). 15 mL of air was sampled using a syringe equipped with a needle and injected into a previously evacuated 12-mL glass vial (Exetainer, Labco Ltd, UK).

To estimate the amount of $^{13}$C that each tree assimilated, the mass (g) of the added $^{13}$C-sodium bicarbonate ($NaHCO_3$) was converted to grams of $CO_2$ added. To estimate uptake efficiency, we subtracted the grams of $^{13}CO_2$ remaining in the tent at the end of the labeling period (obtained from final gas sample) from the total added $^{13}CO_2$ to estimate total uptake. This was then divided by the amount added to obtain a percent uptake efficiency.

## Sample collection

To determine how trees allocated newly assimilated carbon to maintenance and to vegetative and mutualist sinks, we conducted measurements of soil and branch respiration, and we collected leaves, twigs, extrafloral nectar, and ants (Table S1 in Online Resource 1). We define "twigs" as the woody biomass of "branches," which also include leaves

**Table 1** Estimates of the amount of $^{13}CO_2$ assimilated by the experimental trees during labeling

| Tree | Date | Time (GMT + 3) | $^{13}CO_2$ added (g) | $^{13}CO_2$ in tent at the end of labeling (g) | Pulse-labeling efficiency (%) |
|---|---|---|---|---|---|
| Uninvaded open | 9-Mar-2020 | 07:12–12:00 | 2.80 | 0.04 | |
| | 10-Mar-2020 | 06:50–11:55 | 6.73 | 1.14 | |
| | | | **8.35** | | **87.7** |
| Uninvaded exclosure | 7-Mar-2020 | 07:30–11:15 | 7.41 | 0.73 | |
| | 7-Mar-2020 | 14:10–17:13 | 2.80 | 0.66 | |
| | | | **8.82** | | **86.4** |
| Invaded open | 11-Mar-2020 | 06:45–11:30 | 6.99 | 0.54 | |
| | 12-Mar-2020 | 07:30–11:30 | 3.60 | 0.36 | |
| | | | **9.69** | | **91.5** |
| Invaded exclosure | 13-Mar-2020 | 07:10–12:50 | 6.99 | 0.39 | |
| | 13-Mar-2020 | 13:50–14:50 | 0.42 | 0.24 | |
| | | | **6.78** | | **91.5** |

"Uninvaded" sites have not been invaded by *P. megacephala*; "invaded" sites have been invaded by *P. megacephala*. Open trees are located outside of the exclosure and thereby exposed to large herbivores; exclosure trees are protected from herbivores within the large-herbivore exclosure

Bold numbers represent the total $^{13}CO_2$ added and pulse-labeling efficiency for each tree

and "stem" as all the woody biomass of a tree. Bole tissue was not collected. Our initial sampling plan was cut short due to the COVID-19 global pandemic (see Table S1 in Online Resource 1 for a complete list of sample sizes). The following samples were collected before the government-mandated return of American team members to the USA: respiration and tissue sampling for all trees 24 and 48 h after the second labeling event and again after 96 h only for trees in the uninvaded plots. Leaves were also collected immediately after removing the labeling tent from each experimental tree (time = 0), and additional leaf samples were collected by Kenyan team members at 60, 90, and 180 days after labeling, and twigs were sampled again at 60 and 90 days after labeling (Table S1 in Online Resource 1).

Vegetative samples were collected as follows. Leaves and twigs were sampled from branches pointing in each of the four cardinal directions and then pooled as a single sample for each time point. Spines were separated from twigs and analyzed separately. Tissues were collected directly into liquid nitrogen and then microwaved for 10 s at 600 W within 3 h to stop enzymatic activity (following methods in (Landhäusser et al. 2018)). Tissues were stored in a –20 °C freezer until drying in an oven at 65 °C for 48 h. Dried tissues were homogenized by grinding with 2.8-mm stainless steel balls in a tissue lyser.

To determine whether trees allocated newly assimilated carbon to ant rewards, we sampled extrafloral nectar using methods modified from McKenna and Thomson (1988). See Online Resource 1 for a full description of nectar collection.

To determine whether the $^{13}C$ label was transmitted to ant mutualists and invasive ants, we collected six ants per tree using an aspirator at each sampling time point. Ants were haphazardly collected from among those patrolling the surface of the tree. In uninvaded plots, all ants were *C. mimosae*. In invaded plots, ants were *P. megacephala* and *Tetraponera penzigi*. The latter is a native ant mutualist that can persist in *P. megacephala*-invaded areas (Palmer et al. 2021). *Pheidole megacephala* was found on all four trees in invaded plots, whereas *T. penzigi* was found on the two labeled trees but not on the control trees. *Pheidole megacephala* patrolled trees at lower densities than native ants, making it necessary to pool *P. megacephala* ants across all sampling time points per tree to obtain sufficient sample weights.

To measure allocation of newly assimilated carbon to respiration, soil and branch respiration were measured by collecting gas samples from associated chambers (see also Online Resource 1). For all respiration measurements, gas samples were taken at 10, 20, and 30 min after sealing the chamber, and all samples were analyzed for $CO_2$ concentrations and $\delta^{13}C$.

## Stable carbon isotope analysis

To compare the carbon isotopic composition of labeled and control samples, we analyzed $\delta^{13}C$ at the UC Davis Stable Isotope Facility. Most solid samples were between 1 and 2 mg, except for the extrafloral nectar, which was between 0.1 and 0.3 mg. All solid samples were combusted on a PDZ Europa ANCA-GSL elemental analyzer interfaced to a PDZ Europa 20–20 isotope ratio mass spectrometer (Secron Ltd., Cheshire, UK). Gas samples were analyzed using a Thermo Scientific GasBench system interfaced to a Thermo Scientific Delta V Plus isotope ratio mass spectrometer (Thermo Scientific, Bremen, Germany). The $\delta^{13}C$ values for all samples are expressed relative to the VPDB (Vienna Pee Dee Belemnite) international standard.

To calculate the isotopic signature of the soil and branch $CO_2$ efflux within the respiration chambers, we used the intercept ($a$) of the Keeling plot relationship (Keeling 1958), which provides an estimate of the isotopic signature of all respiratory sources in the soil and branch chambers:

$$\delta^{13}C \text{ in } CO_2 \text{ efflux} = \delta^{13}C \text{ in } CO_2 \text{ sample} + a \times \left( \frac{1}{CO_2 \text{ concentration sample}} \right)$$

Samples with Keeling plots with an $R^2 < 0.9$ were not used.

## Statistical analysis

Statistical analyses were conducted in R (R Core Team 2021) (version 4.1.1) and the R studio interface (RStudio Team 2020). An important caveat throughout is that our sample sizes are limited. Means are reported ± SE.

To determine how abiotic variables influenced net uptake of $CO_2$ by trees, we conducted Pearson correlation tests between the rate of change in tent $CO_2$ concentrations and (1) photosynthetically active radiation (PAR, μmol $m^{-2}$ $s^{-1}$) and (2) heat index (HI, °C) (see also Online Resource 1).

To assess the success of labeling, we compared tree tissue from control and labeled trees using Mann–Whitney $U$ tests because the data violated assumptions of normality and homoscedasticity. To assess differential allocation of newly assimilated sugars to different tissues, we used a general linear mixed model from the *glmmTMB* package (Brooks et al. 2017) to predict $\delta^{13}C$ in tree vegetative samples. We used plant material and time of sampling as fixed factors and accounted for sampling over time using tree identity as a random intercept. To determine the best model, we conducted model selection in the MuMIn

package (Barton 2019). To conduct multiple comparisons among the different plant materials, we used Tukey's HSD in the emmeans package (Lenth 2022).

Next, we explored the $\delta^{13}C$ in ants. First, we compared plant materials and ants because ants from uninvaded plots consume tree-derived nectar. To do this, we averaged the $\delta^{13}C$ values of each plant material and of ants from each tree, across all sampling times, to simplify our model. We then used a linear model to test for differences in average $\delta^{13}C$ among plant vegetative samples and ants. Multiple comparisons were conducted using Tukey's HSD in the emmeans package (Lenth 2022). Second, ants from the uninvaded plots (*C. mimosae*) were compared between control and labeled trees using a Kruskal–Wallis test. The ants from the invaded plots could not be compared statistically, given unique replicates for *P. megacephala* and a lack of control for *T. penzigi.*

To compare the $\delta^{13}C$ signature from respiration among control trees, labeled trees, and atmospheric samples, we used a Kruskal–Wallis test and Dunn's post hoc test because the data were non-normal and heteroscedastic.

To estimate the total relative allocation of new photosynthate to different carbon sinks at the tree level, we scaled atom percent $^{13}C$ in samples to estimates of relative mass of the $^{13}C$ label allocated to the stem tissues and ant mutualists of the whole tree. We estimated whole-tree relative allocation to the stem and ants using allometric equations based on tree height and main stem diameter (see Equation S3, S4, and methods in Online Resource 1). For stem relative allocation estimates, we used the 48-h post-label samples. For ants, due to sample availability, we primarily used the 24-h post-label samples.

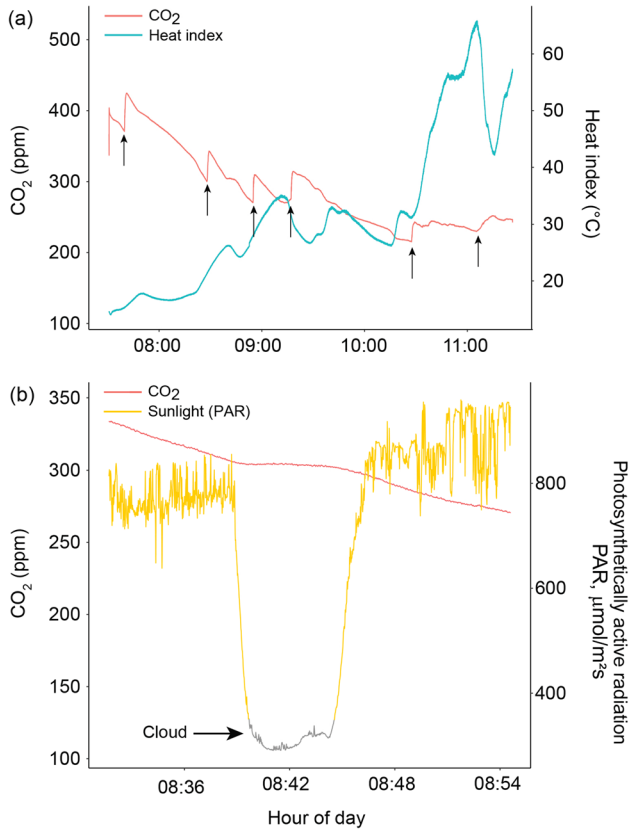


**Fig. 2** Carbon dioxide ($CO_2$) concentration and environmental variables inside of the labeling tent during labeling. **a** The $CO_2$ concentration and heat index (calculated from temperature and relative humidity) inside of the labeling tent during the first labeling event for the uninvaded exclosure tree. Arrows show additions of $^{13}CO_2$. **b** The $CO_2$ concentration and photosynthetically active radiation (PAR) in the chamber during the first labeling event for the uninvaded exclosure tree. For PAR, yellow indicates full sun, while gray shows a cloud passing over

## Results

### Labeling success

All four labeled trees received similar amounts of $^{13}CO_2$ (8.4 ± 0.6 g), with an average estimated uptake efficiency of 89.3 ± 0.01% (Table 1). $CO_2$ concentration in the tent declined after each $^{13}CO_2$ addition, indicating photosynthetic uptake by the tree exceeded above-ground plant respiration (Fig. 2a). The overall downward trend in tent $CO_2$ concentration over the duration of the labeling period was due to the IRGA bias against the progressively higher relative concentration of $^{13}CO_2$ as we added additional pulses of $^{13}CO_2$. Although we thus were not able to track the total $CO_2$ concentration in the tent very accurately, final tent $CO_2$ concentrations (438 ± 17 ppm) did not differ from atmospheric concentrations (412 ± 14 ppm).

Net $CO_2$ assimilation between $^{13}CO_2$ pulses was highest in full sunlight and stopped completely when the heat index grew too high inside the labeling tent (Fig. 2). Overall, the rate of net $CO_2$ uptake was positively correlated with photosynthetically active radiation (PAR) ($r = 0.67$, df = 27, $P < 0.001$). Interestingly, $CO_2$ uptake via photosynthesis barely balanced $CO_2$ release via respiration when clouds obscured the sun (PAR < 400 µmol $m^{-2}$ $s^{-1}$) (Fig. 2b). Heat index had a marginal negative impact on net $CO_2$ uptake ($r = -0.25$, df = 27, $0.2 > P > 0.1$). Visually, there appeared to be an upper threshold for each tree (heat index = 32–55 °C), where high heat indices were associated with an end to net assimilation (Fig. 2a and S1 in Online Resource 1).

### Relative sink-level C allocation

We detected variable allocation of the $^{13}C$ from pulse labeling to solid tree tissues (Fig. 3). The labeling treatment increased $\delta^{13}C$ in all tree tissues and associated ants relative to control trees during the early chase period (1–4 days

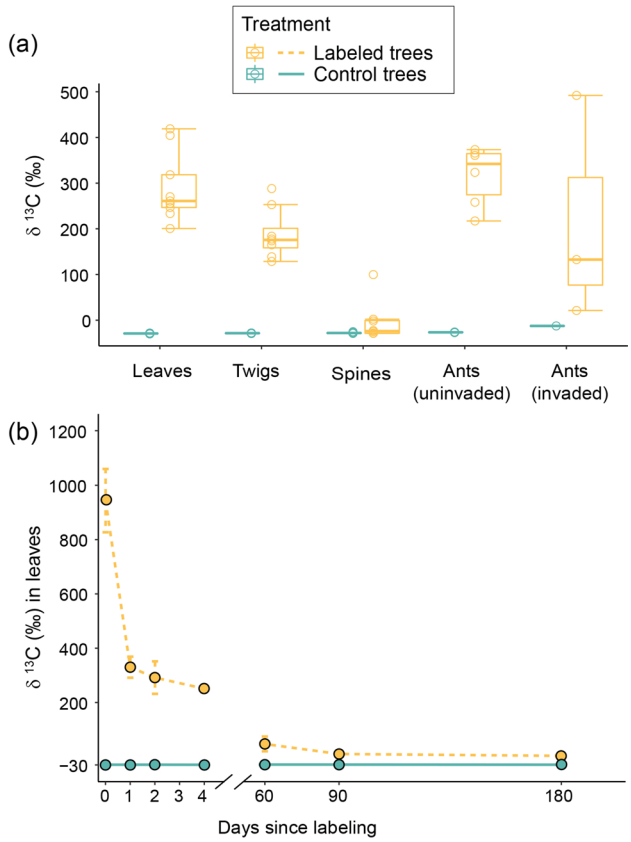


**Fig. 3** $^{13}$Carbon (C) in solid samples from labeled and unlabeled control trees. **a** Box plots showing the quantiles and raw data for early time points (24 h, 48 h, and 96 h) of $^{13}$C in solid samples from labeled and control trees. **b** Mean δ$^{13}$C per mil in leaves at all of the sampling time points. Bars indicate standard errors; bars that are not visible had standard errors <5‰. For time 0, only leaves from the second labeling event are included

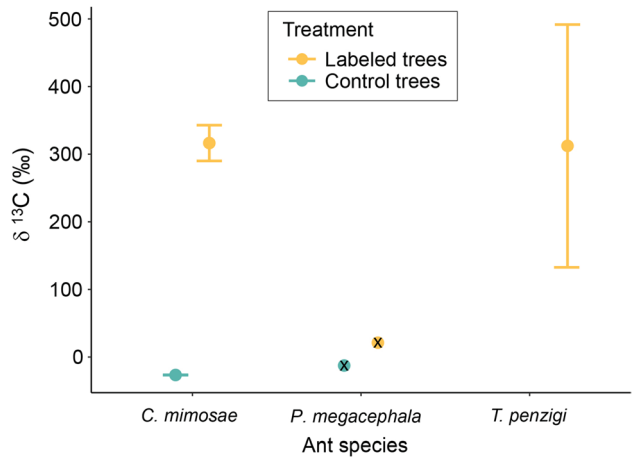


**Fig. 4** Mean $^{13}$C in ant species, pooled for all time points. Bars represent the standard error and an *x* through a point indicates $n=1$. Sample sizes varied because samples were pooled across trees when necessary to achieve the minimum weights required for analysis. *T. penzigi* was not present on control trees

post-label) ($W=60$, $P<0.0001$, Fig. 3a). The amount of $^{13}$C in the early chase period also varied among tissues of labeled trees ($\chi^2=189.2$, df = 2, $P<0.0001$), with the highest δ$^{13}$C in leaves (289.9 ± 25.3‰) and the lowest δ$^{13}$C in spines (−4.2 ± 15.5‰).

Native *C. mimosae* ants from labeled trees had a similar mean δ$^{13}$C (316.5 ± 26.4‰) to leaves from labeled trees and a higher δ $^{13}$C than twigs and spines from labeled trees ($P<0.05$; Fig. 3a). Extrafloral nectar also appeared to receive labeled carbon: δ$^{13}$C of extrafloral nectar was higher in labeled trees (17.8‰) than in control trees (−20.5‰). The isotopic signature of $^{13}$C in leaves of labeled trees declined nearly 65% within the first day of the chase period, before leveling off over the following 3 days (Fig. 3b). A $^{13}$C signal was detected in leaves up to 180 days after labeling (Fig. 3b). In twigs from labeled trees, δ $^{13}$C was consistent 1–4 days after labeling (188.6 ± 19.4); twig δ$^{13}$C then declined by 55% between 4 and 60 days after labeling but was still detectable up to 90 days after labeling (Figure S2 in Online Resource 1).

The $^{13}$C signature from the pulse was variable among ant species, but native ants appear to have used more recent plant-derived C from the label than the invasive *P. megacephala* (Fig. 4). In the uninvaded plots, *C. mimosae* from labeled trees had a much higher isotopic signature than *C. mimosae* from control trees ($H=7.5$, df = 1, $P=0.006$, Fig. 4). Nevertheless, in the invaded plots, *P. megacephala* from labeled trees also contained 21.18‰ δ$^{13}$C, compared to −12.58 ‰ δ$^{13}$C on control trees. The δ$^{13}$C in *P. megacephala* from control trees was higher than in *C. mimosae* ants from control trees (−12.58‰ ($n=1$) versus −26.59 ± 0.46‰). There was considerable variation in δ$^{13}$C in *T. penzigi* from the two labeled trees (312.3 ± 179.7‰), with one sample containing more plant-derived C from the pulse label than the *C. mimosae* from labeled trees and the other less.

There was a clear signature of the pulse label emerging from both branch and soil respiration (Fig. 5). Branch $^{13}CO_2$ efflux was higher 24 h after labeling than 48 h after labeling but was still higher 48 h after labeling in the labeled trees than in control trees (1043.2 ± 305.5‰ versus −17.26; Fig. 5a). $^{13}CO_2$ in branch efflux was different among labeled trees, control trees, and atmospheric samples ($W=18.1$, df = 2, $P=0.0001$). In post hoc comparisons, control branch efflux also differed from labeled branch efflux ($P<0.0001$). Soil $^{13}CO_2$ efflux from labeled trees was highest 12 h after the pulse (16.5‰) and was then relatively constant from 1 to 4 days after labeling (Fig. 5b). Soil $CO_2$ efflux also differed among labeled trees, control trees, and atmospheric samples

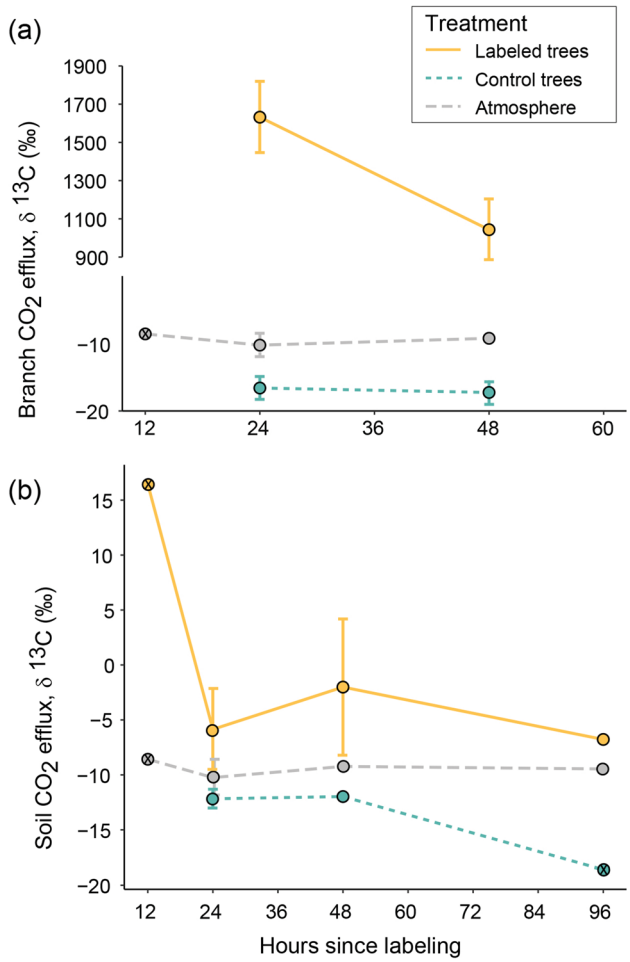


**Fig. 5** Isotopically enriched carbon dioxide ($^{13}CO_2$) from aboveground (branch) and belowground (soil) efflux. **a** The amount of $^{13}CO_2$ in branch efflux for labeled and control trees. Note the *y*-axis breaks and changes in scales. **b** The amount of $^{13}CO_2$ in soil efflux for labeled and control trees. In both (**a**) and (**b**), points represent sample means, bars represent standard errors, and an x through a point indicates $n = 1$. Missing values at sampling times are due to $R^2$ values for Keeling plots <0.9

($H = 14.2$, df = 2, $P = 0.0008$), and control tree soil differed from labeled tree soil in post hoc comparisons ($P = 0.005$).

### Relative tree-level C allocation

The uninvaded, herbivore-exposed tree appeared to allocate almost twice as much newly assimilated C to the stem than either the uninvaded, herbivore-excluded tree or the invaded, herbivore-exposed tree at 48 h after labeling (Table 2). Invasion by *P. megacephala* and simulated herbivore loss, meanwhile, appeared to produce similar changes in the relative allocation of new C to the stem at 48 h after labeling (20–25% compared to 40% in the uninvaded, herbivore-exposed tree; Table 2).

**Table 2** Relative (%) tree-level carbon allocation to stems and ants for each labeled tree

| Invaded by *P. megacephala* | Vertebrate herbivory | Stem (%) | Ants (%) |
|---|---|---|---|
| Uninvaded | Yes | 45 | 1.20 |
| | No | 20 | 0.20 |
| Invaded | Yes | 25 | 0.09 |
| | No | NA | 0.03 |

Stem investment estimates are based on samples collected 48 h after labeling. Due to experimental error, there were no twig samples from the invaded tree inside the fence. Ant allocation estimates are based on samples collected at 24 h after labeling, except for the invaded tree with herbivory, where the 24-h and 48-h samples were combined to meet the minimum weight for isotope analysis. At the invaded site, only allocation to *T. penzigi* ants is estimated, because we do not have allometric equations to estimate the biomass of tree-associated *P. megacephala*

The native mutualist ant *C. mimosae* appeared to receive approximately six times more newly assimilated C on the tree exposed to herbivores than on the tree protected from herbivores. Similarly, even in the invaded plots, the native mutualist ant *T. penzigi* appeared to receive approximately three times more newly assimilated C on the tree exposed to herbivores than on the tree protected from herbivores. *Crematogaster mimosae* in uninvaded plots received relatively more newly assimilated C than *T. penzigi* in invaded plots.

## Discussion

In this pilot study, we demonstrated that adult *A. drepanolobium* trees can be pulse labeled with $^{13}CO_2$ in situ, allowing us to track newly assimilated C to plant sinks and ant mutualists. The $^{13}C$ label was recovered in all pools that we measured, providing evidence that the newly assimilated C was transported throughout the tree within 24 h after labeling. During labeling events, temperature and humidity in the labeling tent rose above ambient conditions, eventually causing $^{13}CO_2$ uptake to stop. However, we were still able to label each tree with the targeted amount of $^{13}CO_2$. Our preliminary results suggest possible differences in newly assimilated C allocated to the stem and ants between trees in invaded and uninvaded plots and between trees exposed to and excluded from herbivores.

This pilot study provides some insight into the physiology of *A. drepanolobium* trees, which seem to operate under strict hydraulic constraints in these semi-arid tropical savannas (Milligan et al. 2022). When the photosynthetically active radiation dropped to ~300 μmol $m^{-2}$ $s^{-1}$ due to cloud cover, net photosynthesis stopped. Stomatal guard cells may close during periods of low light, which would limit water loss. Although we did not continuously measure ambient

temperature in this experiment, our data from inside the labeling tent indicate that temperatures inside the tent may have reached 6–16 °C above the predicted ambient maximum temperature for our location (24.75 °C, (Harris et al. 2014)) before net $CO_2$ uptake stalled. Although high experimental temperatures are a liability of labeling adult trees in exposed tropical environments, our experiment demonstrates that closed-tent approaches are still feasible for introducing enough $^{13}C$ to trees at the equator that can last at least up to 180 days post-label. Nevertheless, the increased temperatures that trees experienced in the labeling tent could affect later C allocation (Rehschuh et al. 2022). In future studies, increased temperatures in the labeling tent could be managed by limiting labeling to shorter time periods or controlled by exposing control trees to similar temperature increases.

Our pulse-labeling efficiency estimates of nearly 90% are similar to those in a labeling study of adult beech trees in a temperate forest (Plain et al. 2009), where the approach of subtracting the amount of $^{13}CO_2$ left in the tent at the end of labeling from the known amount of label added was also used. In that study, the authors also estimated labeling efficiency by measuring the amount of $^{13}C$ in the leaves immediately after labeling and scaling up to the biomass of all leaves on the tree. This approach yielded a slightly lower efficiency estimate of ~75%, similar to estimates (60%) in a study of tropical montane trees (Shibistova et al. 2012). The leaf biomass approach may frequently yield efficiency estimates that are lower than the gas estimate approach, perhaps because of the rapid translocation of fixed $^{13}C$ sugars from the leaves to other parts of the plant. In the next iteration of this experiment, we plan to use both the gas and leaf biomass approach to assess if our estimates are consistent with existing literature for both estimates.

Labeled C was clearly found in all three species of ants associating with *A. drepanolobium* trees. The large quantities of $^{13}C$ label we found in *C. mimosae* ants is probably due to their consumption of large quantities of labeled tree nectar. Although we are not sure why the nectar itself appeared to contain less $^{13}C$ than the *C. mimosae* ants, there are at least two possibilities. First, the labeled nectar sample was pooled over 4 days post-labeling, which may have obscured temporal variation in nectar $^{13}C$. For example, we may have diluted an early-biased signal by pooling these samples. Second, the labeled nectar sample contained less carbon than the smallest reference sample in the analysis, meaning that the $^{13}C$ in this sample could have been underestimated. Native *T. penzigi* ants, which persist in *P. megacephala*-invaded savannas, also appeared to have consumed tree $^{13}C$, with the caveat that we were missing ants from unlabeled control trees for this species. Although *T. penzigi* does not consume nectar, these ants may instead consume fungi from inside the domatia of their host trees (Baker et al. 2017). Further research is needed to understand the extent to which these domatia-associated fungi might rely on tree carbon and how such transfer might occur. We expected to see little to no $^{13}C$ label in *P. megacephala* because, to our knowledge, the ants of this species do not directly consume tree tissue. The presence of a slight signal could be due to *P. megacephala* consuming insect herbivores feeding on the leaves or roots of labeled trees (Loke and Lee 2004). *Pheidole megacephala* from control trees also had an elevated $\delta\ ^{13}C$ signal compared to *C. mimosae* from control trees. Differences in $\delta^{13}C$ in ant species from control trees could be due to differences in diet: *C. mimosae* strongly relies on plant-derived extrafloral nectar (Palmer et al. 2008), whereas *P. megacephala* is more omnivorous (Loke and Lee 2004).

As we predicted, tree rewards for native protective ant partners appeared to be reduced in the absence of herbivores, at least at 48 h after labeling. For *C. mimosae*, this could be driven by plastic allocation to nectar by the tree, where selection could favor limiting C rewards to protective ants when the threat of herbivory is low (Palmer et al. 2008). Although we observed the same pattern in *T. penzigi*, the mechanism is less clear because we do not know the extent to which the fungi that appear to sustain *T. penzigi* colonies depend on tree C transfer.

Our study demonstrates that $^{13}C$ tracer experiments are feasible in the tropics and can be utilized to investigate C allocation to plant–animal interactions. Our limited results suggest potential differences in C allocation by tropical trees due to biotic interactions other than herbivory, which are not often considered, and which may be particularly important in the tropics (Schemske et al. 2009). Additionally, we have shown that we can use $^{13}C$ tracer experiments to track C allocation belowground, which includes important pools for C storage in tropical savannas (Zhou et al. 2022).

In conclusion, *A. drepanolobium* trees and the savanna systems they dominate exhibit substantial potential for studying tree C allocation to tree mutualists and in the context of biotic interactions. We have shown that $^{13}C$ pulse labeling can be used effectively in situ because the tree tolerates labeling-tent conditions for extended periods of time, allowing the uptake of sufficient labeled $^{13}C$ to be detected in all measured pools and up to at least 180 days post-label. Potential differences in C allocation and relative investment were detected, but further investigation with replication is needed to understand the effect of these global change drivers on individual-level C allocation and its consequences for these savanna systems.

**Supplementary Information** The online version contains supplementary material available at https://doi.org/10.1007/s11258-023-01350-0.

**Acknowledgements** We thank the Kenyan government (NACOSTI/P/20/4126, NACOSTI/P/20/3255) for their permission to conduct this project. We also thank the Ol Pejeta Conservancy for logistical support, with special thanks to Samuel Mutusya, Benard

Gituku, and Nelly Jepkirui. We thank Jacob Goheen and Corinna Riginos for their contributions to setting up the experimental plots. We are grateful to Susan Trumbore, Mariah Carbone, and Jay Arnone for all of their insights.

**Author contributions** EGP and TMP conceptualized the study, and EGP, GMM, and TK designed the methods. BWS provided methods and resources for gas sampling and analysis. GMM, EGP, TMP, TK, JSL, and JM performed the experiments. GMM conducted statistical analysis advised by EGP. GMM led the writing of the manuscript, and EGP, BWS, and TMP contributed to revisions.

**Funding** This work was supported by grants from the U.S National Science Foundation to EGP (NSF DEB-1935498) and TMP (NSF DEB-1556905).

**Data availability** Data are available from Dryad: https://doi.org/10.5061/dryad.h9w0vt4q4

## Declarations

**Conflict of interest** The authors have no relevant financial or non-financial interests to disclose.

## References

Baker CCM, Martins DJ, Pelaez JN, Billen JPJ, Pringle A, Frederickson ME, Pierce NE (2017) Distinctive fungal communities in an obligate African ant–plant mutualism. Proc R Soc B Biol Sci 284(1850):20162501. https://doi.org/10.1098/rspb.2016.2501

Bakker ES, Ritchie ME, Olff H, Milchunas DG, Knops JMH (2006) Herbivore impact on grassland plant diversity depends on habitat productivity and herbivore size. Ecol Lett 9(7):780–788. https://doi.org/10.1111/j.1461-0248.2006.00925.x

Barton K (2019) MuMIn: multi-model inference (R package version 1.43.6) [Computer software]. https://CRAN.R-project.org/package=MuMIn

Brooks ME, Kristensen K, van Benthem KJ, Magnusson A, Berg CW, Nielsen A, Skaug HJ, Mächler M, Bolker BM (2017) GlmmTMB balances speed and flexibility among packages for zero-inflated generalized linear mixed modeling. R J 9(2):378–400

Burns CE, Collins SL, Smith MD (2009) Plant community response to loss of large herbivores: comparing consequences in a South African and a North American grassland. Biodivers Conserv 18(9):2327–2342. https://doi.org/10.1007/s10531-009-9590-x

Dirzo R, Young HS, Galetti M, Ceballos G, Isaac NJB, Collen B (2014) Defaunation in the Anthropocene. Science 345(6195):401–406. https://doi.org/10.1126/science.1251817

Epron D, Ngao J, Dannoura M, Bakker MR, Zeller B, Bazot S, Bosc A, Plain C, Lata JC, Priault P, Barthes L, Loustau D (2011) Seasonal variations of belowground carbon transfer assessed by in situ $^{13}CO_2$ pulse labelling of trees. Biogeosciences 8(5):1153–1168. https://doi.org/10.5194/bg-8-1153-2011

Epron D, Bahn M, Derrien D, Lattanzi FA, Pumpanen J, Gessler A, Hogberg P, Maillard P, Dannoura M, Gerant D, Buchmann N (2012) Pulse-labelling trees to study carbon allocation dynamics: a review of methods, current knowledge and future prospects. Tree Physiol 32(6):776–798. https://doi.org/10.1093/treephys/tps057

Goheen JR, Palmer TM (2010) Defensive plant–ants stabilize megaherbivore-driven landscape change in an African savanna. Curr Biol 20(19):1768–1772. https://doi.org/10.1016/j.cub.2010.08.015

Harris I, Jones PD, Osborn TJ, Lister DH (2014) Updated high-resolution grids of monthly climattic observations—the CRU TS3.10 Dataset. Int J Climatol 34:623–642. https://doi.org/10.1002/joc.3711

Hartmann H, Trumbore S (2016) Understanding the roles of nonstructural carbohydrates in forest trees—from what we can measure to what we want to know. New Phytol 211(2):386–403. https://doi.org/10.1111/nph.13955

Hocking B (1970) Insect associations with the swollen thorn acacias. Trans R Entomol Soc Lond 122(7):211–255. https://doi.org/10.1111/j.1365-2311.1970.tb00532.x

Huang J, Hammerbacher A, Weinhold A, Reichelt M, Gleixner G, Behrendt T, van Dam NM, Sala A, Gershenzon J, Trumbore S, Hartmann H (2019) Eyes on the future—evidence for trade-offs between growth, storage and defense in Norway spruce. New Phytol 222(1):144–158. https://doi.org/10.1111/nph.15522

Huang J, Hammerbacher A, Gershenzon J, van Dam NM, Sala A, McDowell NG, Chowdhury S, Gleixner G, Trumbore S, Hartmann H (2021) Storage of carbon reserves in spruce trees is prioritized over growth in the face of carbon limitation. Proc Natl Acad Sci 118(33): e2023297118. https://doi.org/10.1073/pnas.2023297118

Keeling CD (1958) The concentration and isotopic abundances of atmospheric carbon dioxide in rural areas. Geochim Cosmochim Acta 13(4):322–334. https://doi.org/10.1016/0016-7037(58)90033-4

Kiers ET, Palmer TM, Ives AR, Bruno JF, Bronstein JL (2010) Mutualisms in a changing world: an evolutionary perspective. Ecol Lett 13(12):1459–1474. https://doi.org/10.1111/j.1461-0248.2010.01538.x

Kristensen JÅ, Rousk J, Metcalfe DB (2020) Below-ground responses to insect herbivory in ecosystems with woody plant canopies: a meta-analysis. J Ecol 108(3):917–930. https://doi.org/10.1111/1365-2745.13319

Landhäusser SM, Chow PS, Dickman LT, Furze ME, Kuhlman I, Schmid S, Wiesenbauer J, Wild B, Gleixner G, Hartmann H, Hoch G, McDowell NG, Richardson AD, Richter A, Adams HD (2018) Standardized protocols and procedures can precisely and accurately quantify non-structural carbohydrates. Tree Physiol 38(12):1764–1778. https://doi.org/10.1093/treephys/tpy118

Lenth RV (2022) emmeans: estimated marginal means, aka least-squares means (R package version 1.8.0.) [Computer software]. https://CRAN.R-project.org/package=emmeans

Loke P-Y, Lee C-Y (2004) Foraging behavior of field populations of the big-headed ant, *Pheidole megacephala* (Hymenoptera: Formicidae). Sociobiology 43(2):9

Malhi Y (2010) The carbon balance of tropical forest regions, 1990–2005. Curr Opin Environ Sustain 2(4):237–244. https://doi.org/10.1016/j.cosust.2010.08.002

McKenna MA, Thomson JD (1988) A technique for sampling and measuring small amounts of floral nectar. Ecology 69(4):1306–1307. https://doi.org/10.2307/1941289

Milligan PD, Martin TA, Pringle EG, Prior KM, Palmer TM (2022) Symbiotic ant traits produce differential host-plant carbon and water dynamics in a multi-species mutualism. Ecology n/a(n/a): e3880. https://doi.org/10.1002/ecy.3880

Nuckolls AE, Wurzburger N, Ford CR, Hendrick RL, Vose JM, Kloeppel BD (2009) Hemlock declines rapidly with hemlock woolly adelgid infestation: impacts on the carbon cycle of Southern Appalachian forests. Ecosystems 12(2):179–190. https://doi.org/10.1007/s10021-008-9215-3

Orians CM, Thorn A, Gómez S (2011) Herbivore-induced resource sequestration in plants: why bother? Oecologia 167(1):1–9. https://doi.org/10.1007/s00442-011-1968-2

Palacio S, Paterson E, Hester AJ, Nogués S, Lino G, Anadon-Rosell A, Maestro M, Millard P (2020) No preferential

carbon-allocation to storage over growth in clipped birch and oak saplings. Tree Physiol 40(5):621–636. https://doi.org/10.1093/treephys/tpaa011

Palmer TM, Young TP, Stanton ML (2002) Burning bridges: priority effects and the persistence of a competitively subordinate acacia-ant in Laikipia, Kenya. Oecologia 133(3):372–379. https://doi.org/10.1007/s00442-002-1026-1

Palmer TM, Stanton ML, Young TP, Goheen JR, Pringle RM, Karban R (2008) Breakdown of an ant–plant mutualism follows the loss of large herbivores from an African savanna. Science 319(5860):192–195. https://doi.org/10.1126/science.1151579

Palmer TM, Riginos C, Milligan PD, Hays BR, Pietrek AG, Maiyo NJ, Mutisya S, Gituku B, Musila S, Carpenter S, Goheen JR (2021) Frenemy at the gate: invasion by *Pheidole megacephala* facilitates a competitively subordinate plant ant in Kenya. Ecology 102(2):e03230. https://doi.org/10.1002/ecy.3230

Plain C, Gerant D, Maillard P, Dannoura M, Dong Y, Zeller B, Priault P, Parent F, Epron D (2009) Tracing of recently assimilated carbon in respiration at high temporal resolution in the field with a tuneable diode laser absorption spectrometer after in situ (CO2)-C-13 pulse labelling of 20-year-old beech trees. Tree Physiol 29(11):1433–1445. https://doi.org/10.1093/treephys/tpp072

Pringle EG (2016) Integrating plant carbon dynamics with mutualism ecology. New Phytol 210(1):71–75. https://doi.org/10.1111/nph.13679

Pringle EG, Akçay E, Raab TK, Dirzo R, Gordon DM (2013) Water stress strengthens mutualism among ants, trees, and scale insects. PLOS Biol 11(11):e1001705. https://doi.org/10.1371/journal.pbio.1001705

R Core Team (2021) R: a language and environment for statistical computing [computer software]. R Foundation for Statistical Computing, Vienna, Austria. https://www.R-project.org/

Rehschuh R, Rehschuh S, Gast A, Jakab A-L, Lehmann MM, Saurer M, Gessler A, Ruehr NK (2022) Tree allocation dynamics beyond heat and hot drought stress reveal changes in carbon storage, belowground translocation and growth. New Phytol 233(2):687–704. https://doi.org/10.1111/nph.17815

Riginos C, Karande MA, Rubenstein DI, Palmer TM (2015) Disruption of a protective ant–plant mutualism by an invasive ant increases elephant damage to savanna trees. Ecology 96(3):654–661. https://doi.org/10.1890/14-1348.1

RStudio Team (2020) RStudio: integrated development for R [computer software]. RSudio, PBC, Boston, MA. http://www.rstudio.com/

Schemske DW, Mittelbach GG, Cornell HV, Sobel JM, Roy K (2009) Is there a latitudinal gradient in the importance of biotic interactions? Annu Rev Ecol Evol Syst 40(1):245–269. https://doi.org/10.1146/annurev.ecolsys.39.110707.173430

Schmitz OJ, Wilmers CC, Leroux SJ, Doughty CE, Atwood TB, Galetti M, Davies AB, Goetz SJ (2018) Animals and the zoogeochemistry of the carbon cycle. Science 362(6419):eaar3213. https://doi.org/10.1126/science.aar3213

Shibistova O, Yohannes Y, Boy J, Richter A, Wild B, Watzka M, Guggenberger G (2012) Rate of belowground carbon allocation differs with successional habit of two Afromontane trees. PLoS ONE 7(9):e45540. https://doi.org/10.1371/journal.pone.0045540

Stanton ML, Palmer TM (2011) The high cost of mutualism: effects of four species of East African ant symbionts on their myrmecophyte host tree. Ecology 92(5):1073–1082. https://doi.org/10.1890/10-1239.1

Trumbore S (2006) Carbon respired by terrestrial ecosystems—recent progress and challenges. Glob Change Biol 12(2):141–153. https://doi.org/10.1111/j.1365-2486.2006.01067.x

Vandenkoornhuyse P, Mahé S, Ineson P, Staddon P, Ostle N, Cliquet J-B, Francez A-J, Fitter AH, Young JPW (2007) Active root-inhabiting microbes identified by rapid incorporation of plant-derived carbon into RNA. Proc Natl Acad Sci 104(43):16970–16975. https://doi.org/10.1073/pnas.0705902104

Villar N, Medici EP (2021) Large wild herbivores slow down the rapid decline of plant diversity in a tropical forest biodiversity hotspot. J Appl Ecol 58(11):2361–2370. https://doi.org/10.1111/1365-2664.14054

Wahungu GM, Mureu LK, Kimuyu DM, Birkett A, Macharia PG, Burton J (2011) Survival, recruitment and dynamics of *Acacia drepanolobium* Sjøstedt seedlings at Ol Pejeta Conservancy, Kenya, between 1999 and 2009. Afr J Ecol 49(2):227–233. https://doi.org/10.1111/j.1365-2028.2010.01254.x

Zhou Y, Singh J, Butnor JR, Coetsee C, Boucher PB, Case MF, Hockridge EG, Davies AB, Staver AC (2022) Limited increases in savanna carbon stocks over decades of fire suppression. Nature 603(7901): Article 7901. https://doi.org/10.1038/s41586-022-04438-1